Topological Analysis of Chaos Characteristics in a Power System

Shan-Ying Li*, Sang-Seung Lee and Jong-Keun Park***

Abstract - This paper proposes a totally new method in the chaos characteristics' analysis of power systems, the introduction of topological invariants. Using a return histogram, a bifurcation graph was drawn. As well, the periodic orbits and topological invariants – the local crossing number, relative rotation rates, and linking number during the process of period-doubling bifurcation and chaos were extracted. This study also examined the effect on the topological invariants when the sensitive parameters were varied. In addition, the topological invariants of a three-dimensional embedding of a strange attractor were extracted and the result was compared with those obtained from differential equations. This could be a new approach to state detection and fault diagnosis in dynamical systems.

Keywords: chaos, topological invariants, power system

1. Introduction

Loads in a power system have become rather complicated in recent years. It is difficult for the power system to stay in one equilibrium point, and it may sometimes operate beyond the limit of its stability. This situation creates concern regarding the bifurcation and chaotic attractors in practice. Even if the power system is dynamically stable, it can exhibit a bounded, random behavior when the stable operating points are perturbed to the attracting region of chaos. This originates from the nonlinear and deterministic structure of the power system itself but not from random load disturbances [1, 2]. Therefore, chaotic analysis can lead to a clearer understanding of the problem of stability and become a useful technique for the control and operation of power systems. Because the essence of chaos is the strange attractor [3], it is important to study its characteristics.

Currently, there are two main approaches for analyzing the chaotic time series in a dynamical system. They are metric [4, 5] and topological [6-10] approaches. The metric approach is based on the distance between the points in the attractor [6]. In this approach it is customary to compute the fractal dimension, the Lyapnov exponent, and the spectrum singularities, etc. It generally requires a large amount of data and degrades rapidly with additive noise. The topological approach is based on the organization of unstable periodic orbits embedded in the strange attractor [6]. It is responsible for creating a strange attractor using stretching and squeezing mechanisms. Some quantities can present how the periodic orbits are knotted and linked to each other. The extraction of these quantities from the time series data is robust against noise and is independently verifiable [7]. These quantities are defined as topological invariants that are effective in modeling the dynamic system.

This paper is organized as follows. The next section introduces the topological invariants, the local crossing number, the relative rotation rates and the linking numbers, and describes how to extract them from the periodic orbits. In Section 3, the topological invariants in a simple power system are calculated and the stability is analyzed as the parameters are changed. The topological invariants were also extracted directly from the periodic orbits reconstructed from the time series and the result was compared to those computed from the equation. The conclusions are reported in Section 4.

2. Extraction of Topological Invariants

When the system is in a chaotic state, the strange attractor appears to be in disorder. However, this is the result of the superposition of infinite periodic orbits and non-periodic orbits. The skeleton of the strange attractor consists of infinite periodic orbits. The following computation of topological invariants is based on the periodic orbits extracted from the strange attractor.

2.1 Local Crossing Number

The local crossing number is the number of half-twists of the period-doubled orbit along the tubular neighborhood [9]. It is an important index that describes the period-doubled process. As an example, an illustration of a

* School of Electrical Engineering, 301-Dong, Seoul National University, Korea. (leeyanjin0202@hotmail.com, parkjk@snu.ac.kr)
** Electrical Engineering and Science Research Institute (EESRI), 130-Dong, Seoul National University, Korea. (sslee@er.snu.ac.kr)
Received May 6, 2003 ; Accepted February 18, 2004

sequence of period-doubling bifurcation is shown in Fig. 1 (from Fig. 2 in Ref. [9]) to explain the local crossing number. The sequence begins with an orbit having a period of one (see Fig. 1a). Its tubular neighborhood is provided in Fig. 1b. After the first period-doubling bifurcation, the 2^1-period orbit sits on the surface of the tubular neighborhood as illustrated in Fig. 1c. The number of half twists of the doubled orbit along the tubular neighborhood is 3. Therefore, its local crossing number C_1 is 3. In this case, the number of crossings of the projected orbit in Fig. 1d is equal to the local crossing number C_1. The above method can be used to calculate local crossing number of the 2^2-periodic orbit as well as the other periodic doubling orbits.

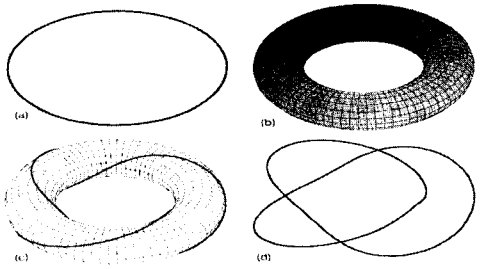

Fig. 1 A sequence of period-doubling bifurcation

The local crossing numbers increase during the process of period doubling. Simultaneously, there is a recurring relationship among the local crossing number of the continuous period-doubling orbits

$$C_{n+2} = C_{n+1} + 2C_n \tag{1}$$

where C_n stands for the local crossing number of the 2^n periodic orbit.

2.2 Relative Rotation Rates – RRR (Self-Relative Rotation Rates – SRRR) and Linking Number – L (Self-Linking Number – SL)

The topological organization of all the unstable periodic orbits extracted from the time series is determined by calculating the relative rotation rates and linking the numbers of all pairs of periodic orbits, the self-relative rotation rates and self-linking number of each individual periodic orbit.

The RRR describe how often one orbit rotates around another on average [6]. They are defined as follows: Two orbits A and B, of periods p_A and p_B, intersect a Poincare section in the p_A and p_B points, respectively. A difference vector between one of the intersections of A and one of the intersections of B with the Poincare section is the propagated forward in time. As it evolves, this difference vector rotates in a plane transverse to the propagation direction. Eventually it will return to its initial position (after p_Ap_B period). This requires an inter rotation through 2π radians. The relative rotation rate, for this pair of initial conditions, is this integer divided by the number of periods, or the average rotation per period. The sum of the RRR notes over all the pairs of initial conditions is the linking number that links the two periodic orbits [6].

Calculating the RRR by the definition above is quite difficult. Ref. [6] introduces a new method for determining the RRR using a permutation matrix P and crossing matrix C, where matrix P describes the forward time evolution of the system and matrix C describes how the orbit segments cross over each other. Furthermore, matrix RRR and L (A,B) between a period, p, and an orbit, A, and a period, q, and an orbit, B, can be defined as

$$2 * p * q * RRR = \sum_{k=0}^{p*q-1} ((P^T)^k * C * P^k) \tag{2}$$

$$L(A,B) = \sum_{i=1}^{p} \sum_{j=1}^{q} R_{i,j}(A,B) \tag{3}$$

Note that the RRR can provide the phase information lacking in the linking numbers. The topological properties are closely linked to physical processes and are often insensitive to noise changes, which are advantages in modeling the system [7].

3. Extraction and Analysis of Topological Invariants in a Simple Power System

This section presents the topological properties of the double-periodic bifurcation and chaos on a detailed model.

3.1 A Simple Power System

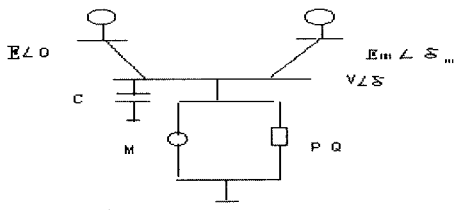

Fig. 2 A simple three-bus system

Consider the power system shown in Fig. 2, which consists of a load that is supplied by two generators [1]. An induction motor in parallel with a constant PQ load is used to represent the load. The equation of this system consists of four state variables that correspond to the generator angle (δ_m), the generator angular velocity (ω), the angle (δ) and the magnitude (V) of the load voltage. The load reactive

power is chosen as the system parameter, so that increasing Q_1 corresponds to increasing the load reactive power demand. Ref. [1] provides detailed system equations of this model. In this paper, all the angles were measured in radians and all the variables and constants are reported in per unit.

$$\dot{\delta}_m = \omega \tag{4}$$

$$M\dot{\omega} = -D\omega + P_m + V_m V Y_m \sin(\delta - \delta_m - \theta) + V_m^2 Y_m \sin\theta_m \tag{5}$$

$$k_{q\omega}\dot{\delta} = -k_{qv}V - k_{qv_2}V^2 + Q - Q_0 - Q_1 \tag{6}$$

$$Tk_{q\omega}k_{pv}\dot{V} = k_{p\omega}k_{qv_2}V^2 + (k_{p\omega}k_{qv} - k_{q\omega}k_{pv})V + k_{p\omega}(Q_0 + Q_1 - Q) - k_{q\omega}(P_0 + P_1 - P) \tag{7}$$

3.2 Topological Properties of Double Period Bifurcation

Many studies have found that chaos exists via a period-doubling route in this model (see Ref. [1, 2]). The bifurcation diagram can exhibit the richest qualitative behavior, as shown in Fig. 3, where the phase-space coordinate is taken by sampling the load voltage V when δ crosses the oscillation center in the decreasing direction. Fig. 3 shows that the power system is stable near Q_1 =11.39. As Q_1 is slowly decreased, the period 2 orbit grows at Q_1 =11.3885, and then undergoes a sequence of a period-doubling bifurcation, leading to chaos. Fig. 4 presents several stable periodic orbits in the sequence of period doubling discussed above, along with the strange attractor resulting from the period doubling cascade.

The topological invariants extracted from the stable period-doubling orbits are shown in Table 1 and Table 2. The result in Table 1 indicates that that local crossing numbers increase gradually as the period doubles and on the continuous periodic orbits there is an extrapolation relation that has been discussed in Section 2. Since there is a close relationship between the local crossing number and the power spectrum of the orbit, the harmonics components are necessarily increased with periodic doubling, namely, heavy oscillation can occur with the period-doubling bifurcation process.

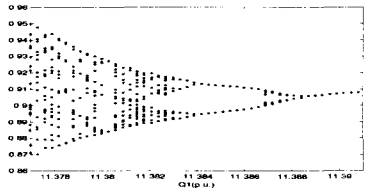

Fig. 3 System bifurcation diagram in the (Q_1, V) plane

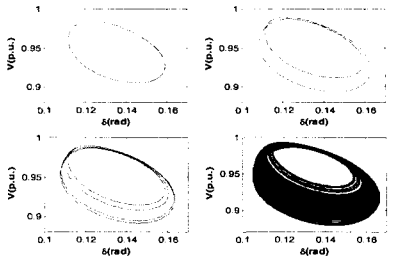

Fig. 4 Period doubling cascade to chaos

Table 1 Local crossing number of period-doubling bifurcation

Period	1	2	4	8
L of δ	0	1	3	5
L of V	0	1	3	5

Table 2 Relative rotation rates and linking numbers of period-doubling bifurcation

Period	1	2	4	8
1	0	-1/2	-1/2	-1/2
2		-1/2,0	-1/2,-1/4	-1/2,-1/4
4			$(-1/2)^2$,-1/4,0	$(-1/2)^2$,-1/4,-3/8
8				$(-1/2)^2$,$(-1/4)^2$,-3/8,0

(a) RRR of period-doubling bifurcation

Period	1	2	4	8
1	0	1	2	4
2		1	3	6
4			5	13
8				23

(b) L of period-doubling bifurcation

For the other two topological invariants, we note that, the self-RRR of the period 1 orbit is 0 and the RRR between the period 1 orbit and the other orbits, the Inter-RRR, have the same value, −1/2. The self-RRRs of the period 2 orbit are 0 and −1/2, which include the self-RRR and the inter-RRR of period 1. Simultaneously, the inter-RRR of the period 2 orbit has the same values, −1/2 and −1/4. Furthermore, the self-RRR of the period 4 orbit contains not only the entire self-RRR of the period 1 and 2 orbits but also new information, −1/4. For the period 8 orbit, the conclusion is similar.

Not much information could be obtained from the linking-number in Table 2(b). This is because the linking number consists of a sum of the RRR on the arbitrary original condition, which often offsets some information.

From the above analysis it can be seen that the topological properties of period 2^n contain all of the topological information in the period 1, 2,..., 2^{n-1} orbits and the larger the period the richer the information that can be observed. This means that the orbit structure from period 1 to period 2^n can be determined if the period 2^n orbit twist is known.

3.3 Topological Characteristics in Chaos State

In section 2 it can be seen that once the hyperbolic structure of chaos is defined, there is a one to one correspondence between the periodic orbits and the flow, namely, the topological invariants. Therefore, if the topological invariants change, the structure of the strange attractor also changes. As such, different chaos attractors can be identified.

For the forth order model, chaos is observed in the approximate range Q_l=11.377-11.382 (see Fig. 3). In order to extract the unstable period orbit in the strange attractor, the fundamental period needs to be determined first. From Fig. 5 we can obtain the fundamental periodic of the unstable period orbit at Q_l=11.379, which is approximately 2.1s according to the relationship between T and ω, $\omega=2\pi/T=2.99$, which is the imaginary part of the complex eigenvalues at Q_l=11.379. The unstable period orbits can then be extracted (see Fig. 6) and the topological invariants can be calculated (see Tab. 3).

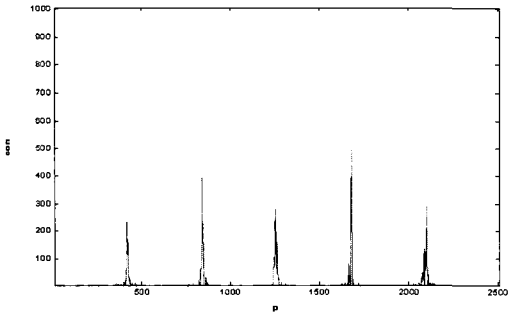

Fig. 5 The return histogram at Q_l=11.379

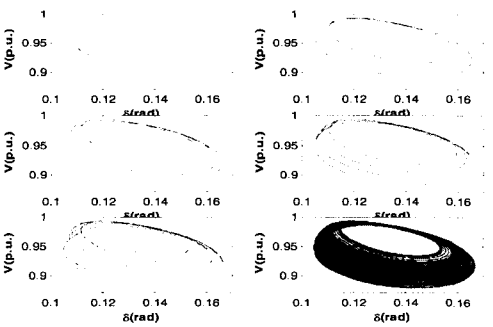

Fig. 6 Extraction of period orbit at Q_l=11.379

Indeed there is another chaos region induced from the period-doubling bifurcation around Q_l=10.89 [1] (fundamental period T=1.67s). The region corresponding to Q_l=10.89 is referred to as the left chaos; the region corresponding to Q_l=11.379 is known as the right chaos. The topological invariants of the left chaos are shown in Table 4.

The results in Table 3 and Table 4 are apparently different, namely, the topological organization of two attractors are different. This means that the characteristic of the two attractors will change as Q_l is varied. In Ref. [1], it is noted that the attractor in the left chaos region will disappear as Q_l is increased, while the attractor in the right chaos region will lead to a voltage collapse as Q_l is decreased. Conversely, the results in Table 3 and Table 4 suggest that the topological invariants are sensitive to changes in the parameter and system structure, which will contribute to the system state detection and fault diagnosis.

Table 3 Relative rotation rates and linking numbers at Q_l=10.89

Period	1	2	3	4	6
1	0 -1/2	-1/3	-1/4	-1/3	
2	-1/2,0	-1/3	-1/4	-1/3,-1/6	
3		$(-1/3)^2$,0	-1/4	$(-1/3)^2$,-1/6	
4			$(-1/4)^3$,0	-1/4,-1/6	
6				$(-1/3)^2$,$(-1/6)^3$,0	

(a) Relative rotation rates

Period	1	2	3	4	6
1	0	1	1	1	2
2		1	2	2	3
3			2	3	5
4				3	5
6					7

(b) Linking number

Table 4 Relative rotation rates and linking numbers at Q_l=11.379

Period	1	2	3	4	6
1	0 -1/2	-1/3	-1/2	-1/3	
2	-1/2,0	-1/3	-1/2,-1/4	-1/3,-1/6	
3		$(-1/3)^2$,	0 -1/3	$(-1/3)^2$,-1/6	
4			$(-1/2)^2$,-1/4,0	-1/3	
6				$(-1/3)^4$,-1/6,0	

(a) Relative rotation rates

Period	1	2	3	4	6
1	0	1	1	2	2
2		1	2	3	3
3			2	4	5
4				5	8
6					9

(b) Linking number

3.4 Effects of Parameter Changes Upon the System

Firstly, the effect of parameter k_{qv2} on the system is considered.

According to the simulation results, voltage collapse and angle divergence take place when k_{qv2} is varied from 2.090 to 2.098. If a point k_{qv2}=2.092 is chosen in the range, then the corresponding voltage and angle curve can be obtained, as shown in Fig. 7.

Let k_{qv2} vary from 2.098 to 2.114, and draw a system

bifurcation graph (see Fig. 8). It should be noted that, when k_{qv2} is gradually decreased from k_{qv2}=2.114, the system experiences bifurcation and a state of chaos. The topological invariants extracted at k_{qv2}=2.100 and k_{qv2}=2.103 are displayed in Tables 5 and 6. It is easy to see that the topological invariants are almost the same except for the RRR between the period 4 and 6 orbits and the RRR between the period 1 and 6 orbits. Furthermore, the topological invariants extracted from the high period orbit can be used to detect the parameter changes. Note that it does not signify that the higher the period the better the result is. Therefore, how many periods should be extracted depends upon the actual demand.

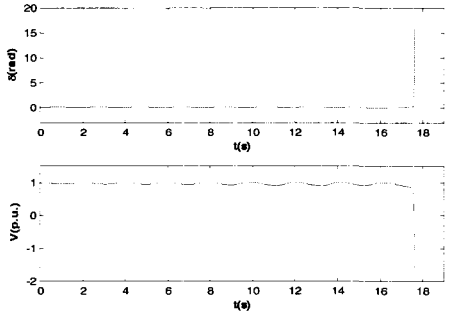

Fig. 7 k_{qv2} leading to voltage collapse and angle divergence

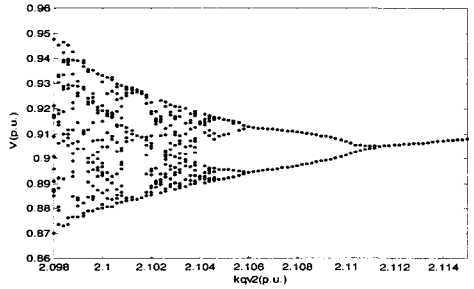

Fig. 8 System bifurcation graph in the (k_{qv2}, V) plane

Table 5 Relative rotation rates and linking numbers at k_{qv2}=2.100

Period	1	2	3	4	6
1	0	-1/2	-1/3	-1/2	-1/3
2		-1/2,0	-1/3	-1/2,-1/4	-1/3,-1/2
3			$(-1/3)^2$,0	-1/3	-1/3
4				$(-1/2)^2$,1/4,0	-1/3,-5/12
6					-1/2,$(-1/3)^4$,0

(a) Relative rotation rates

Period	1	2	3	4	6
1	0	1	1	2	2
2		1	2	3	5
3			2	4	6
4				5	9
6					11

(b) Linking number

In the following we will discuss effects of the other parameters k_{qv}、 k_{pv}、 k_{pw}、 k_{qw} on the voltage (see Fig. 9). Here a brief account regarding Fig. 9 is given. The vertical axis stands for the voltage and the horizontal axis stands for every parameter, whose variable range is (-0.5%k_Δ , +0.5% k_Δ), where k_Δ denotes the parameter k_{qv}、 k_{pv}、 k_{pw}、 k_{qw}. From Fig. 9, it can be seen that, parameter k_{qw}, k_{pv}, k_{pw} has a weak effect on the load voltage (see Fig. 9 (b)-(d)), while load voltage is sensitive to parameter k_{qv}.

Table 6 Relative rotation rates and linking numbers at k_{qv2}=2.103

Period	1	2	3	4	6
1	0	-1/2	-1/3	-1/2	-1/2
2		-1/2,0	-1/3	-1/2,-1/4	-1/3,-1/2
3			$(-1/3)^2$,0	-1/3	-1/3
4				$(-1/2)^2$,1/4,0	-1/3,-1/2
6					$(-1/2)^3$,$(-1/3)^2$,0

(a) Relative rotation rates

Period	1	2	3	4	6
1	0	1	1	2	3
2		1	2	3	5
3			2	4	6
4				5	10
6					13

(b) Linking number

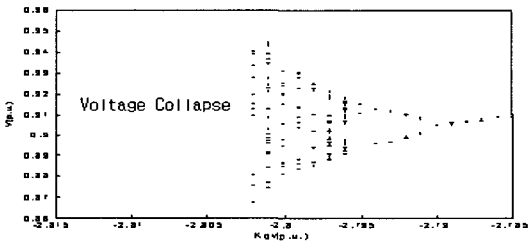

(a) Effect of parameter k_{qv} on the voltage

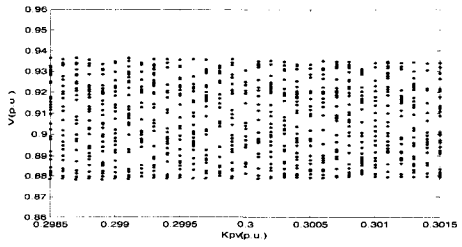

(b) Effect of parameter k_{pv} on the voltage

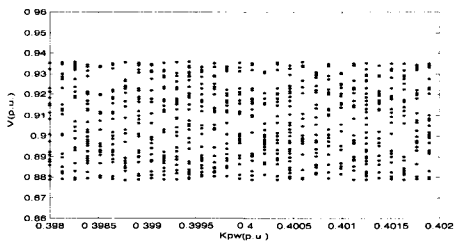

(c) Effect of parameter k_{pw} on the voltage

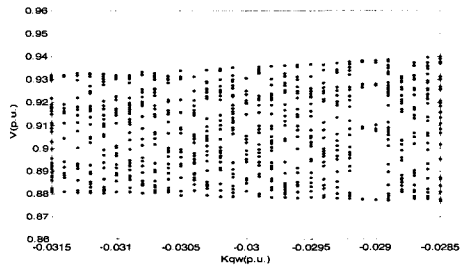

(d) Effect of parameter k_{qw} on the voltage

Fig. 9 The effect of the parameters on the voltage

The analysis given above demonstrates that k_{qv} and k_{qv2} are sensitive parameters of the system because even subtle changes can lead to a different state - stable, period oscillation, chaos, collapse, where the chaos state can be thought of as a transition process from the stable to unstable state. Parameter k_{qv2} is the coefficient in front of V^2 in equations (8) and (9), which suggest that the coefficients of the non-linear term in the model have the dominant influence on the stability. Therefore, it is important for operators to examine the equipments concerned with these sensitive parameters. Once their changes exceed the regulated range, appropriate actions must be taken in order to avoid a large fault such as a voltage collapse.

Although the topological invariants method is mainly used to analyze the doubling-period bifurcation and chaos, it is also an effective way to deal with a non-stable process.

3.5 Topological Characteristics from Time Series

The topological invariants discussed above are extracted from the forth order model. If a model of the power system is not known precisely, and only the measurement data is available, i.e. time series, then the topological invariants can still be extracted. This section will discuss this.

First, it is postulated that the system model is unknown and only the time series V(t) of the magnitude of the terminal voltage, which is the simulation results at Q_1=11.379, is available. Because the topological invariants cannot be described unless a three-dimensional embedding can be found, a three-dimensional embedding of the strange attractor needs to be constructed. An integral-differential filter is constructed [6], which is easily implemented by an electronic circuit and reduces the S/N (Signal/Noise) ratio.

$$Y_1(i) = \sum_{j<i} V(j) e^{-(i-j)/\tau} \tag{8}$$

$$Y_2 = V(i) \tag{9}$$

$$Y_3(i) = V(i+1) - V(i-1) \tag{10}$$

The reconstructed attractor in R^3 is shown in Fig. 10. Fig. 11 depicts the fundamental period of the attractor (T=2.1s). The attractor is projected on the phase-phase Y2-Y3 and the unstable periodic orbits in it are extracted (see Fig. 12).

The topological invariants, shown in Table 7, can then be calculated. It can be seen that the result is the same as that presented in Table 4. However, we cannot be sure that the topological organization of the two attractors (one is from the time series and the other from the model) is equivalent. The identity of the topological invariants is not the necessary sufficient condition for the same topological organization. In order to identify whether the two attractors are equivalent, further research using template and symbolic dynamics theory will be needed.

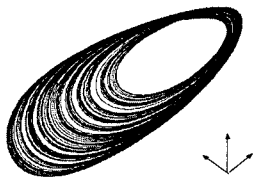

Fig. 10 Embedding of the strange attractor

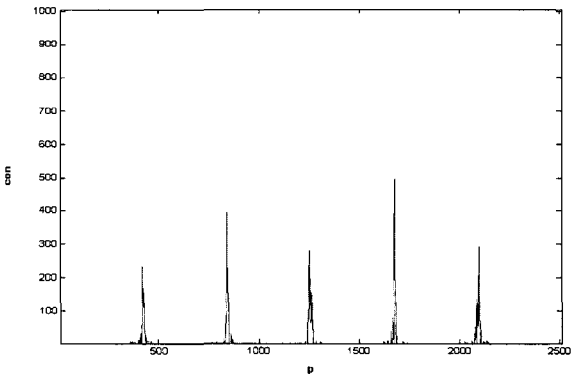

Fig. 11 The return histogram

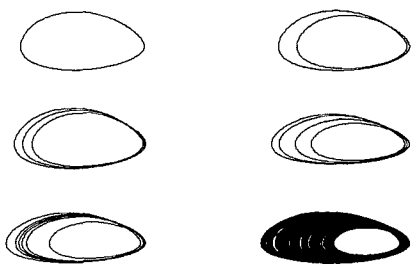

Fig. 12 Extraction of the period orbit at Q_1=11.379

Table 7 Relative rotation rates and linking numbers

Period	1	2	3	4	6
1	0	-1/2	-1/3	-1/2	-1/3
2		-1/2,0	-1/3	-1/2,-1/4	-1/3,-1/6
3			$(-1/3)^2$,0	-1/3	$(-1/3)^2$,-1/6
4				$(-1/2)^2$,-1/4,0	-1/3
6					$(-1/3)^4$,-1/6,0

(a) Relative rotation rates

Period	1	2	3	4	6
1	0	1	1	2	2
2		1	2	3	3
3			2	4	5
4				5	8
6					9

(b) Linking number

It is more appropriate to analyze the chaotic behavior as a function of time than by the model in practice. The discussion in this section is more suitable for diagnosing a fault in a practical power system.

4. Conclusion

This study analyzed the topological characteristics of a simple power system. The analysis of the topological invariants during period-doubling bifurcation show that the period 2^n orbit contains all the topological information of the previous periodic orbits (period 1, 2, 2^2,..., 2^{n-1} orbits). Moreover, the larger n is, the richer the topological information that can be obtained. The topological invariants can identify the attractor belonging to the different chaos regions and the oscillation period can be easily obtained by a return map and a return histogram. A three-dimensional embedding was successfully constructed from the time series, and topological invariants of time series were found to be the same as those of the fourth-differential equations. It is useful to analyze the characteristic of a power system from a practical perspective when a fault takes place. Comparing the results to other topological invariants, the relative rotation rates suggest the wealth of information, which is responsible for creating a strange attractor. Therefore, the RRR can be taken as a sensitive factor in a fault diagnosis since they indicate whether or not the two dynamic systems are equal. Note that the topological invariants are only sensitive to a parameter variation that leads to qualitative changes in the system, while they are insensitive for the quantitative changes in the system.

In future works, it is hoped that the dynamics (stretching and squeezing mechanisms) can be modeled by a horse-holder template and symbolic dynamics theory based on the topological invariants extracted from the model or the experimental data sets. That would be a more appropriate and effective approach for studying the dynamics rather than the metric approach.

In addition, although this study focused on chaos via the period-doubling bifurcation route, the method discussed above is still valid for other routes that approach chaos.

Acknowledgements

This work has been supported in part by EESRI, which is funded by MOCIE (Ministry of Commerce, Industry and Energy).

References

[1] H. D. Chiang, C. C. Liu, etc. "*Chaos in a Simple Power System*", IEEE Trans. Power Systems, vol.8, no.4, pp.1407-1417, 1993.

[2] K.G. Rajesh and K.R. Padiyar, "*Bifurcation Analysis of a Three Node Power System With Detailed Models*", Elect. Power and Energy System, vol.21, pp.375-393, 1999.

[3] E. N. Lorenz, *The Essence of Chaos*, Beijing, China, 1997.

[4] P. Grassberger and I. Procaccia, "*Estimation of the Kolmogorov Entropy from a Chaotic Signal*", Phys. Rev. A, vol.28, pp.2591-2593, 1983.

[5] A. Wolf, J. B. Swift, H. L. Swinney and J. A. Vastano, "*Determining Lyapunov Exponents from a Time Series*", Physica D, vol.16, pp.285-317, 1985.

[6] G. B. Mindlin, H. G. Solari, M. A. Natiello, R. Gilmore and X. J. Hou, "*Topological Analysis of Chaotic Time Series Data from the Belousov-Zhabotinskii Reaction*", J. Nonlinear Sci., vol.1, pp.147-173, 1991.

[7] G. B. Mindlin and R. Gilmore, "*Topological Analysis and Synthesis of Chaotic Time Series*", Physica D , vol.58, pp.229-242, 1992.

[8] H. G. Solari and R. Gilmore, "*Relative Rotation Rates for driven dynamical systems*", Physical review A, vol.8, no.37, pp.3096-3109, 1988.

[9] T. Motoike, T. Arimitsu and H. Konno, "*A Universality of Period Doublings-local Crossing Number*", Physics Letter A, vol 182, pp.373-380, 1993.

[10] T. Arimitsu and T. Motoike, "*A Universality of Period Doubling Bifurcations*", Physica D, vol.84, pp.290-302, 1995.

[11] Bo-Ju Jiang , "*Mathematics of String Fig.s*", Hunan, China, 1998.

Shan-Ying Li

She was born in Jinlin Province, China, on March 29, 1975. She received her B.S. degree in Computer Science and M.S. degree in Electrical Engineering from the Northeast China Institute of Electric Power Engineering, China in 1997 and 2002, respectively. She is currently pursuing a Ph.D. degree in the School of Electrical Engineering at Seoul National University. Her research interests are in the areas of non-linear control of power systems.

Sang-Seung Lee

He was born in Goseong, Gyeongnam, Korea on April 2, 1960. He received his Ph.D. degree from the School of Electrical Engineering at Seoul National University, Seoul, Korea in 1998. Currently, he is the Research Leader of the Power System Research Division (PSRD) of the Electrical Engineering and Science Research Institute (EESRI), 130-Dong, Seoul National University, Seoul, Korea. His interest lies in the areas of power system interconnections, control, power system economics and power distribution system plans.

Jong-Keun Park

He was born in Youseong, Chung cheongnam-Do, Republic of Korea, on October 21, 1952. He received his B.S. degree in Electrical Engineering from Seoul National University, Seoul, Korea in 1973 and his M.S. and Ph.D. degrees in Electrical Engineering from The University of Tokyo, Japan in 1979 and 1982, respectively. In 1982, Dr. Park worked as a Researcher at the Toshiba Heavy Apparatus Laboratory. He has been an Associate Professor at Seoul National University since 1983. He is currently a Professor in the School of Electrical Engineering, Seoul National University. In 1992, he was a Visiting Professor at the Technology and Policy Program Laboratory for Electromagnetic and Electronic Systems, Massachusetts Institute of Technology. He is a senior member of the Institute of Electrical and Electronics Engineers (IEEE) and the Japan Institute of Electrical Engineers (JIEE).